Enhanced Background Oriented Schlieren (EBOS)

IOP Conf. Series: Journal of Physics: Conf. Series **1249** (2019) 012017 doi:10.1088/1742-6596/1249/1/012017

Enhanced Background Oriented Schlieren (EBOS)

F. Cozzi[1], E Göttlich[2]

[1] Politecnico Milano, Dipartimento di Energia, Via Lambruschini 4, Milano, Italy
[2] Graz University of Technology. Institute for Thermal Turbomachinery and Machine Dynamics

Email: fabio.cozzi@polimi.it

Abstract. The Background Orientend Schlieren (BOS) is a line of sight optical technique that exploits light refraction arising in inhomogeneous density field to visualize or either measure density gradients. The working principle of BOS is quite simple: a background patter appears distorted when observed through an optical inhomogeneous media, by comparing the distorted and undistorted images the apparent local displacement of the background pattern can be measured. The images comparison is carried out using either cross-correlation or optical flow techniques. In the framework of geometric optics and for a 2D refractive index field the measured displacements is proportional to the refractive index gradient. When applicable, the Gladstone-Dale relationship provides the link between the refractive index and the fluid density. The uncertainty in the measured displacements affects the qualitative and quantitative results extracted from BOS images. Spatial and temporal filtering techniques can reduce the uncertainty at the expenses of the spatial and the temporal resolutions. This work describes a modified BOS technique, named Enhanced BOS (EBOS), which is able to reduce the displacement uncertainty without using any spatial or temporal filter. The EBOS technique uses N undistorted images of a grey-scale background pattern taken at slightly different potions, the N reference images are paired with a single distorted background image. Eventually displacement maps obtained from the N image couples are averaged together. The mean displacement map is an improved estimate of the actual displacement field. The EBOS technique can also be used with optical flow techniques anyhow we limited our investigation to image analysis based on cross-correlation technique. The paper reports the results obtained by applying EBOS and BOS techniques to the same test case. The comparison evidence the capability of EBOS to reduce displacement uncertainty respect to BOS by using a limited number of undistorted background images. EBOS and BOS techniques achieve almost the same uncertainty when the number of particles contained in an interrogation area is high, thus EBOS is most advantageous to use when small interrogation area are required.

1. Introduction

The Background Orientend Schlieren (BOS) is a line of sight optical technique that exploits light refraction arising in inhomogeneous density field to visualize or either measure density gradients. The technique was described almost simultaneously by Dalziel et al. under the name of “synthetic schlieren” [1] and by Raffel et al. [2] as “background-oriented optical density gradient technique”. An overview of BOS describing typical applications and literature in the field is offered by Raffel [3].

Ray of lights traversing a transparent inhomogeneous optical medium are subjected to refraction, this causes a background pattern to appears distorted when observed through the inhomogeneous field. Being the refractive index and the fluid density related through the Gladstone-Dale relationship [4] any spatial density variation gives rise to an inhomogeneous optical field (as occurring for example in compressible flows or in flow with inhomogeneous thermal fields). For 2D field and not too strong refraction effects the details of the background appear just displaced by an amount proportional to the local refractive index gradient. The density gradient field is recovered by using the measured displacements, the Gladston-Dale relationship [4] and the geometrical data of the optical set-up. Eventually the density field is computed through integration of a Poisson equation [4, 5]. The uncertainty in displacements data can significantly affects the qualitative and quantitative results extracted from BOS images.

The most simply BOS set-up is composed by a digital camera, an imaging lens, a background pattern, a lighting system and a suitable software tool to analyze the images. Usually the background pattern is an artificially generated random dot pattern arranged in the background of the test volume, other patterns like Gabor noise and multi-scale pattern such as wavelet noise have been used [7][8]. Generally speaking the background pattern preferably has to have the highest spatial frequency that can be imaged with sufficient contrast. In large scale outdoor experiments the natural background can be used as BOS background [9]. Advanced cross-correlation techniques [10] or either optical flow based techniques [8] can be used to extract the displacements fields from BOS images.

The continuous improving in image acquisition and analysis, the ease of use of the technique have contributed to significantly increase the usage and the progress of the BOS technique over the years since its first appearance. As a matter of fact the BOS has been applied to investigate a wide spectra of phenomena: supersonic flows [4, 10], rotor blade tip vortex of a full scale helicopter [12], free flight experiment [13], heat transfer in natural convection [14] and free jet [10] to name just but a few. Recent improvements include the use of telecentric lens [7, 15], of stereoscopic and tomographic configurations [15, 16] and very recently the use of plenoptics camera[18].

Accuracy and spatial resolution of the BOS technique based on image cross correlation have been investigated by Vinnichencko et al [6]. Their results evidence that accuracy is mainly affected by the background pattern, while the interrogation area size set the spatial resolution. Moreover the best performances were achieved using a chaotic patterns with dot size 2 or 3 pixels.

Spatial or temporal filters applied to the measured displacement field can reduce both noise and uncertainty, anyhow this reduces the spatial and the temporal resolution by smearing out or even filtering out sharp spatial and temporal variations. For image cross-correlation based analysis the use of wider interrogation areas increases the signal to noise ratio improving the detection of the correlation peak, once again this came at a price of a lower spatial resolution. To increases BOS accuracy Leopold et al. proposed to use a colored background; the latter is generated by randomly distributing the same proportion of each primary color: red, green and blue, in the background pattern [19]. Up to eight different background images can be extracted from the color image by separating the color planes; the displacement fields obtained by applying a cross-correlation algorithm to each image couple are averaged together so as to reduce the random error [19, 20, 21]. Schroder et al. uses a continuously varying random dot pattern projected by a Digital Mirror Device (DMD) as a background image; accuracy is improved by averaging together the displacement fields found using cross-correlation algorithm and obtained for the changing dot pattern [22]. This method requires steady state conditions and it adds some complexities to the set-up due to the digital projection system. Lastly optical flow techniques have been also applied to BOS images, Atcheson et al. claim the optical flow techniques improve performances of BOS respect to cross-correlation based techniques [8].

This work focuses on an original way to improve the accuracy of displacement estimations in BOS images by using multiple background images paired to one single instantaneous flow image. The proposed technique is named Enhanced Background Oriented Schlieren (EBOS), being not based on spatial or temporal filtering the EBOS technique is able to preserve the details of the displacement field both in time and space. EBOS can be used in combination with optical flow algorithms

nevertheless we purposely limited our study to image analysis based on cross-correlation. The paper describes the EBOS technique and reports a comparison between EBOS and BOS when both applied to the same test case. We analyzed the influence of the number of background images, of the interrogation area size and of particle image density on the uncertainty of the two techniques. The experimental results evidence the capability of EBOS to achieve a smaller uncertainty respect to BOS.

2. The Enhanced Background Oriented Schlieren (EBOS) technique

The Enhanced Background Oriented Schlieren technique (EBOS) makes use of N different undistorted images of a single grey-scale background pattern. Besides the image of the undistorted background in its reference position the other images are taken with the background at a position slightly displaced from the reference one. The displacements need to differ from each other and they have to sum to zero to reduce random errors and to remove bias in the final result. Alternatively the camera (or even the camera sensor) can be displaced while keeping the background at a fixed position, anyhow no significant differences in the results are expected and which approach to choose is just a matter of convenience.

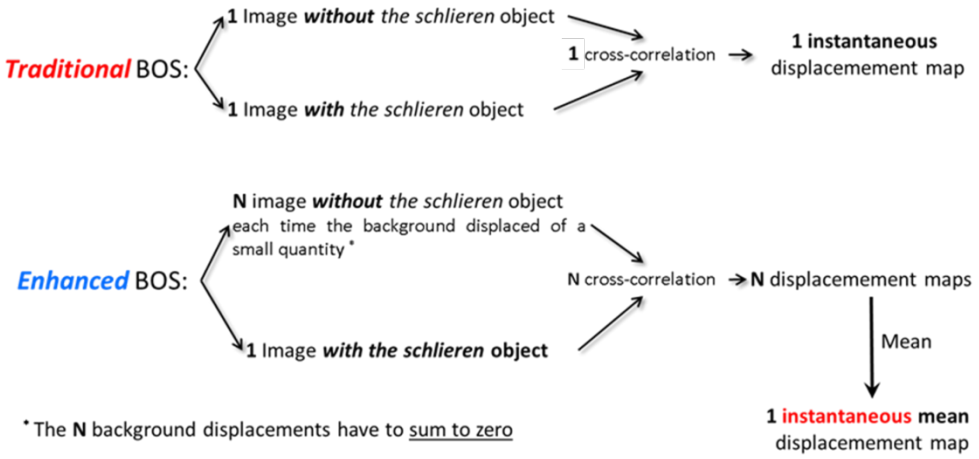

Figure 1. Traditional BOS vs. Enhanced BOS

Each of the N images of the undistorted background are coupled to the single image of the distorted background (i.e. the one taken with the schlieren object in place) and from each couple the apparent displacement map is obtained by using a cross-correlation technique. Eventually the N displacement map are averaged together to reduce the random error and to remove the bias originated by the rigid displacements imposed to the background. Figure 1 summarizes the difference between the standard BOS and the EBOS technique. Actually being the background pattern always the same, the N displacement maps could be more or less correlated, this would limit the uncertainty reduction achievable through their average.

3. Method of testing the Enhanced Background Oriented Schlieren technique

The test the effectiveness of EBOS technique, both EBOS and BOS were applied to the same test case and results compared. To avoid any uncertainty introduced by the use of a schlieren object, the displacement field was generated by simply rotating the background pattern of a small angle, θ, around an axis perpendicular to the background itself. A rotating background has already been used by Michaelis et al. to assess errors of PIV technique [23]. To make a correct comparison, the same identical image of the rotated background was used by BOS and EBOS.

A 2D rigid roto-translation of the background originates a displacement field $\vec{\Delta}(X,Y) = \Delta X\vec{\imath} + \Delta Y\vec{\jmath}$ which is a linear function of the in-plane coordinates X, Y and of the rotation angle θ, see Figure 2. According to equation (1) a point originally at coordinates X and Y is displaced by an amount equal to

ΔX and ΔY along axis X and Y, where $\bar{\bar{\Omega}}$ is the 2D rotation matrix, equation (2), $\bar{\bar{I}}$ is the unit matrix, equation (3), and the vector $\begin{bmatrix} X_0 \\ Y_0 \end{bmatrix}$ takes into account of a rigid displacement.

$$\begin{bmatrix} \Delta X \\ \Delta Y \end{bmatrix} = \{\bar{\bar{\Omega}} - \bar{\bar{I}}\} \begin{bmatrix} X \\ Y \end{bmatrix} + \begin{bmatrix} X_0 \\ Y_0 \end{bmatrix} \tag{1}$$

$$\bar{\bar{\Omega}} = \begin{bmatrix} cos\theta & -sin\theta \\ sin\theta & cos\theta \end{bmatrix} \tag{2}$$

$$\bar{\bar{I}} = \begin{bmatrix} 1 & 0 \\ 0 & 1 \end{bmatrix} \tag{3}$$

In the image plane the displacement field $\vec{\Delta}(x, y) = \Delta x\vec{\imath} + \Delta y\vec{\jmath}$ is given by equation (4), image coordinates x and y are related to corresponding object coordinates X and Y through the lens magnification, M, as per equation (5).

$$\begin{bmatrix} \Delta x \\ \Delta y \end{bmatrix} = \{\bar{\bar{\Omega}} - \bar{\bar{I}}\} \begin{bmatrix} x \\ y \end{bmatrix} + \begin{bmatrix} x_0 \\ y_0 \end{bmatrix} \tag{4}$$

$$\begin{bmatrix} x \\ y \end{bmatrix} = M \begin{bmatrix} X \\ Y \end{bmatrix} \tag{5}$$

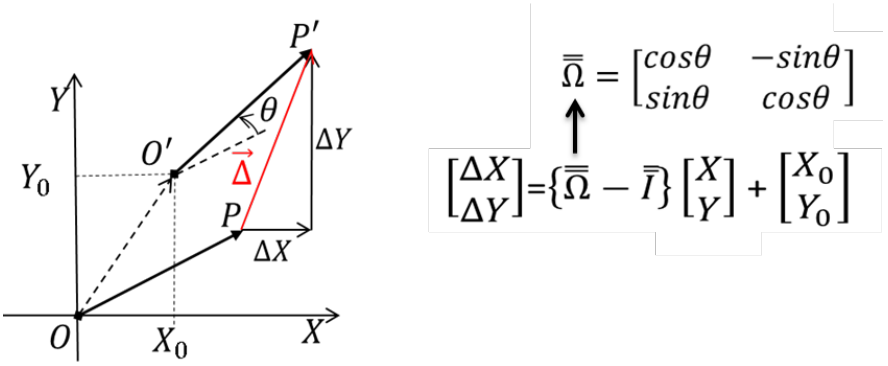

Figure 2. Displacement $\vec{\Delta}(X, Y) = \Delta X\vec{\imath} + \Delta Y\vec{\jmath}$ due to a rigid roto-translation of the background. X and Y are the background in-plane coordinates, θ is the rotation angle and X_0 and Y_0 are a rigid displacement.

At first the background is moved at N different positions and at each position one image of the background is taken, the set of the N positions describe a square grid centred on a fixed reference location, see Figure 3. While random positions could be used, the regular square grid allows to easily satisfy the constrain that displacements have to sum to zero. The picture taken with the background in its reference position and rotated of the small angle θ is paired to each one of the N background images. The N image couple are analyzed using an adaptive cross-correlation algorithm and the resulting N displacement fields are averaged together. Being the sum of the displacements imposed to the background equal to zero, the mean displacement vector field $\bar{\vec{\Delta}}(x, y)$ contains only the displacements originated by the background rotation.

$$\bar{\vec{\Delta}}(x, y) = \frac{1}{N}\sum_{i=1}^{N} \vec{\Delta}_i(x, y) \tag{6}$$

On the other side, the displacement map, $\vec{\Delta}_0(x, y)$, obtained analyzing a single image couple, i.e. composed by the rotated and the un-rotated background at the reference position, is the results of the standard BOS technique.

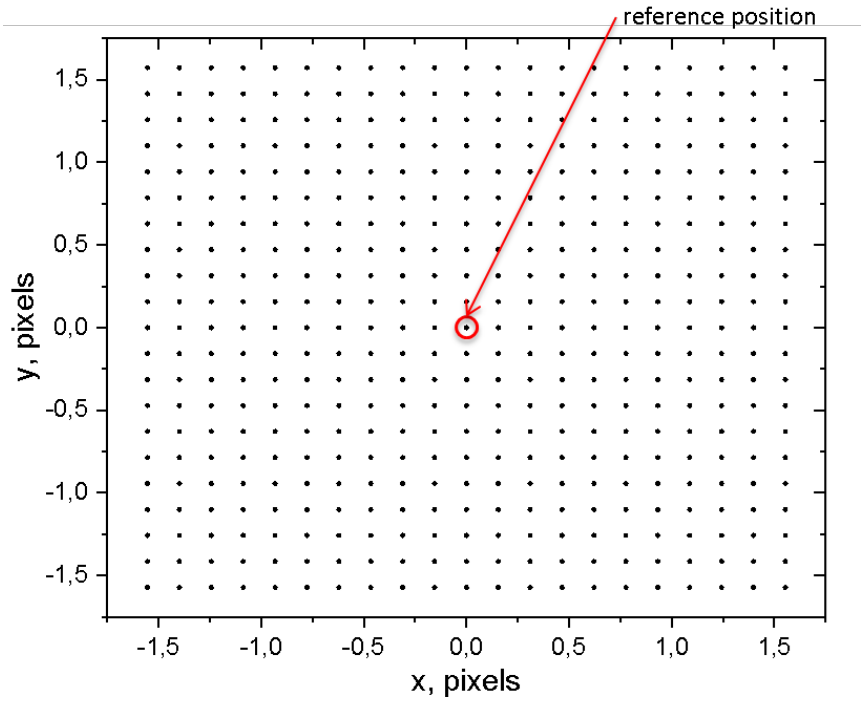

Figure 3. Regular square grid showing (in the image space) the background positions, the point at $x = 0, y = 0$ corresponds to the reference positions. Coordinates are in pixels.

The accuracy of EBOS and BOS techniques is assessed by evaluating the difference between the modulus of the measured displacements, $\|\vec{\Delta}_m(x,y)\| = \sqrt{\Delta x^2 + \Delta y^2}$ and the corresponding values obtained from equation (4). Please keep in mind that for EBOS $\vec{\Delta}_m(x,y) = \bar{\vec{\Delta}}(x,y)$, while for BOS $\vec{\Delta}_m(x,y) = \vec{\Delta}_0(x,y)$. The modulus of the displacement $\|\vec{\Delta}_m(x,y)\|$ can be expressed as per equation (7) where coefficients a, b, c and d are functions of the angle θ and of the rigid translation x_0, y_0:

$$\|\vec{\Delta}_m(x,y)\|^2 = ax^2 + ay^2 + bx + cy + d \tag{7}$$

Actually the value of the above coefficients are not exactly known, thus they are computed by fitting the measured $\|\vec{\Delta}_m(x,y)\|^2$ with the function $ax^2 + ay^2 + bx + cy + d$. The mean square error, ε_{Δ^2}, is estimated according to equation (8), where $\|\vec{\Delta}_m(x_j,y_j)\|$ is the modulus of the displacement measured at position (x_j,y_j) and L is the total number of points in the map. The quantity $(ax_j^2 + ay_j^2 + bx_j + cy_j + d)$ is the theoretical displacement of point (x_j,y_j) due to the rotation θ.

$$\varepsilon_{\Delta^2} = \sqrt{\frac{1}{L}\sum_{j=1}^{L}\left[\|\vec{\Delta}_m(x_j,y_j)\|^2 - (ax_j^2 + ay_j^2 + bx_j + cy_j + d)\right]^2} \tag{8}$$

By expressing displacements and positions in pixels units the error ε_{Δ^2} is in unit of pixels^2. The smaller the value of ε_{Δ^2} the smaller the uncertainty in the measured displacement.

4. Experimental set-up and image analysis procedure

The experimental set-up is shown in Figure 4, it is composed by a monochrome CCD camera having a resolution of 1344x1024 pixels and a pixel pitch of 6.45 µm. A 60 mm lens is attached to the camera and lens aperture is set to $f/8$. The background is lighted by a continuous white LED, an interferential band-pass filter centered at 430 nm and with 10 nm bandwidth is placed in front of the CCD sensors

to remove chromatic aberration from the lens. The optical magnification, M, resulted to be about 0.035, thus in the object space the pixel pitch corresponds to about 0.184 mm.

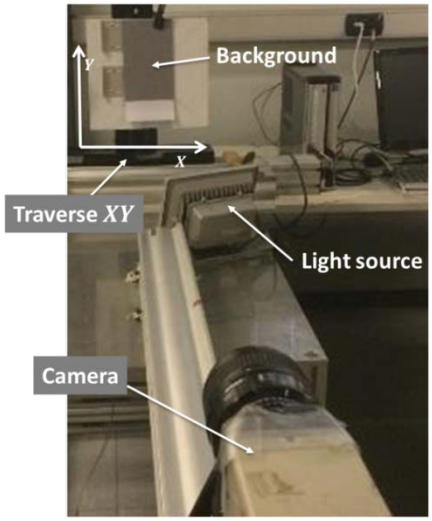

Figure 4. Set-up used to test the accuracy of the EBOS system

The background pattern is made by random white dots printed on a black background, when recorded by the CCD camera the average image dot size was about 3 pixels, this value is in the range of 2-4 pixels suggested by Adrian and Westerweel to minimize both bias and random errors in cross-correlation based algorithm [24]. Particle image density is about 0.037 particle/pixel, which corresponds to about 9 particles for a 16x16 pixels interrogation area size. The background pattern is placed at a distance of about 1770 mm from the camera lens and perpendicularly to its optical axis.

A linear translation system allows to independently displace the background along two perpendicular axis lying in the background plane. The translation system is controlled by a PC through a Labview program, the camera acquisition is controlled in such a way to take one image of the background after each displacement. The translation stage has a minimum step size of 0.1 μm and the on-axis accuracy declared by the manufacturer is 5 μm. The latter corresponds to about $1/37$ of a pixel pitch when project to the CCD sensor plane. The square grid of background displacements is composed of 441 positions, the grid step is about 0.15 pixels and the maximum absolute displacement along both x and y axes is about 1.5 pixels. To check the effect of the number of background displacements 121, 49, 9 and 5 positions where selected among the original 441 positions and corresponding images extracted from the original set of 441.

The background pattern is shown in Figure 5(a) and the image of the about 1° counter clockwise rotated background is shown in Figure 5(b). Image acquisition and analysis are performed using DynamicStudio 4.15 from Dantec Dynamics. To reduce computational time only the portion of the image shown by the red square in Figure 5(a) is analyzed. An adaptive cross correlation algorithm is used to analyze the images. Three different Interrogation Area (IA) sizes are used: 32x32 pixels, 16x16 pixels and 8x8 pixels, the starting IA size is always 64x64 pixels. Two validations criteria are applied in the adaptive algorithm: a) the ratio of the first peak to the second peak in the cross-correlation greater than 1.2, b) local neighbourhood validation on a 3x3 vectors cell size along with a moving average for replacing bad vectors. No further validation is performed on the resulting vectors. The number of substitute vectors is negligible small, less than 0.1% for the worst case. Finally the mean displacements map is computed using both validated and substituted vectors.

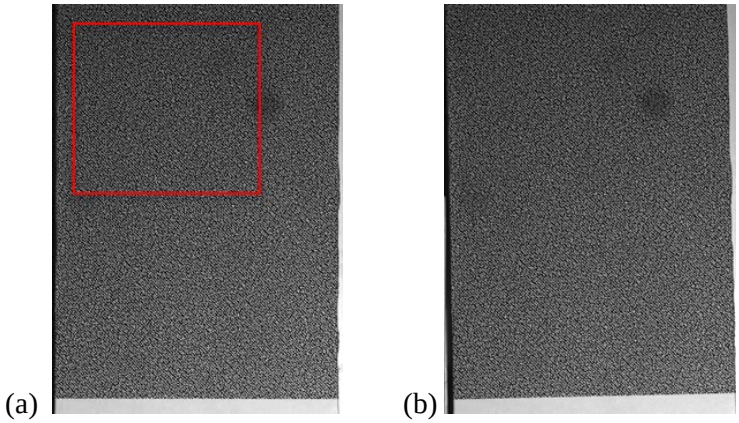

Figure 5. (a) reference background image, the red square shows the analyzed region; (b) background pattern counter-clockwise rotated of about 1°

A typical displacement field $\|\vec{\Delta}(x,y)\|$ obtained from the analysis of a single couple of image is shown in Figure 6. The imposed rigid rotation should give a map of $\|\vec{\Delta}(x,y)\|$ having circular isoline, noise and errors in the cross-correlation and in the subpixel displacement estimation prevents this to occur, Figure 6.

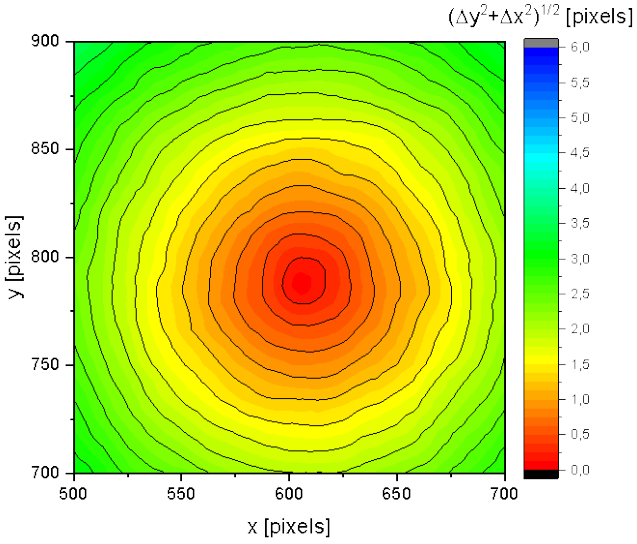

Figure 6. Displacement field $\|\vec{\Delta}(x,y)\|$ obtained from the analysis of a single couple of image. Lines of constant $\|\vec{\Delta}(x,y)\|$ are shown by the thin solid lines.

5. Experimental results

The mean square error was computed according the procedure outlined in the previous section by analysing the single image of the rotated background coupled with $N = 441, 121, 49, 9$, and 5 images of the displaced background. The mean square error obtained for a single image couple: background in its reference position and rotated background (i.e. $N = 1$), it is used as representative of BOS technique. The imposed background rotation estimated from the parameter a of the fitting function, equation (7), resulted to be about 1.3° ($a \cong 5.12 * 10^{-4}$).

The mean square error ε_{Δ^2} is shown in Figure 7 as a function of the number of background images, N, and for IA sizes of 8x8, 16x16 and 32x32 pixels. As already explained, error values for $N = 1$ corresponds to those of standard BOS and they are taken as reference against which evaluate

improvements offered by the EBOS technique. For all the IA sizes a clear reduction in ε_{Δ^2} is observed when N increases from 1 (i.e. standard BOS) to $N = 5$, by increasing N the reduction in ε_{Δ^2} decreases and levels off for $N \geq 49$. By using an IA of 8x8 pixels and EBOS with $N = 5$ the error ε_{Δ^2} is of about 26% smaller than corresponding one for BOS, the difference between the two errors decreases to about 18% and to about 15% when using IA of 16x16 and 32x32 pixels, respectively. Unfortunately errors do not show the $1/\sqrt{N}$ trend expected for uncorrelated data, see Figure 7, this is probably due to the use of a single background pattern which likely generates partially correlated displacement maps.

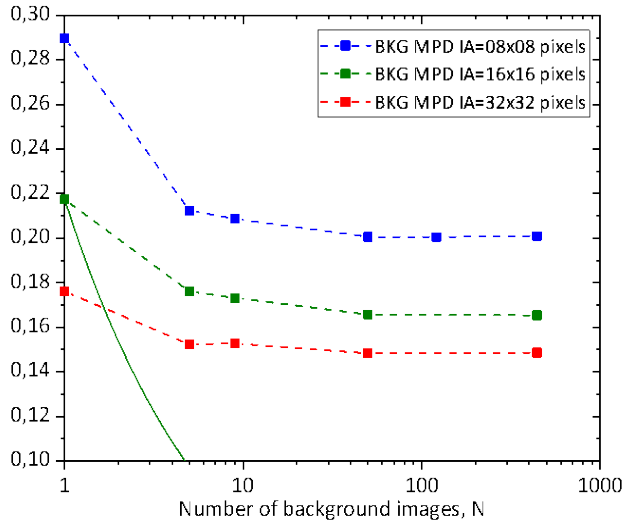

Figure 7. Effect of N and IA size on the root mean square error. The solid line shows the ideal $1/\sqrt{N}$ trend for IA size of 16x16 pixels.

Another interesting result evidenced by Figure 7 is the dependence of ε_{Δ^2} on the IA size. Both BOS ($N = 1$) and EBOS ($N > 1$) techniques show a smaller error, ε_{Δ^2}, when the IA size is increased from 8x8 to 32x32 pixels. Anyhow EBOS shows values of ε_{Δ^2} smaller than the corresponding one for BOS and less affected by the IA size. These behaviours can be better appreciated by plotting ε_{Δ^2} as a function of the interrogation area size, see Figure 8.

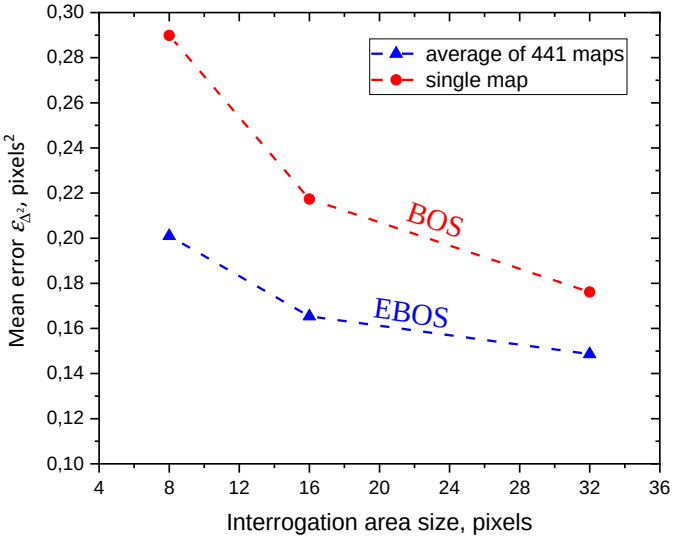

Figure 8. Effect of IA size on the root mean square error for $N = 441$. ● standard BOS, ▲ EBOS with $N = 441$.

Both BOS and EBOS techniques take advantage of the higher number of particles images contained in IA of bigger size (IA of 8x8, 16x16 and 32x32 pixels contains about 2, 9 and 36 particles, respectively), this reduces the uncertainty in the location of cross-correlation peak by improving the cross-correlation signal to noise ratio [25]; nevertheless EBOS shows smaller error as compared to BOS. By increasing the IA size the mean errors of BOS and of EBOS get closer and likely for IA bigger than 32x32 pixels the difference between the two goes to zero, Figure 8. In any case EBOS can achieve almost the same accuracy of BOS by using IA size of a factor four (area ratio) smaller than that used in BOS.

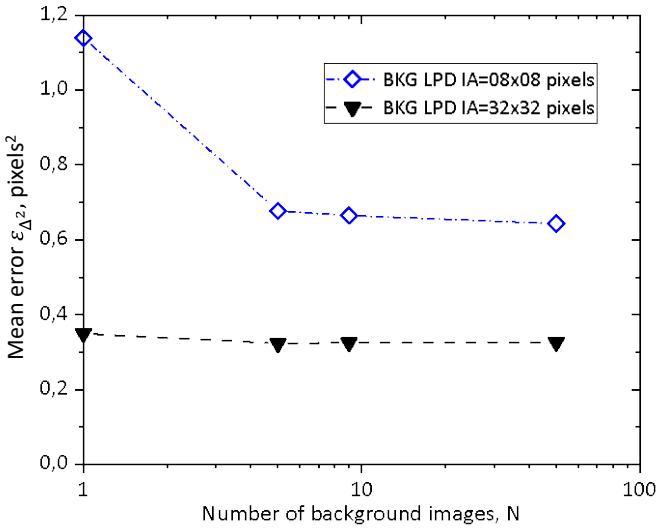

Figure 9. Low particle density background, effect of IA size on the root mean square error.

The previous results evidence the EBOS technique to be most effective in reducing the mean error when the IA size is small, i.e. when the IA contains few particle images, let's say less than ten. To further analyse this aspect experiments have been repeated using a background pattern having a particle density of about 0.011 particles per pixel, corresponding to about 1 particle in a IA of 8x8 pixels and about 11 particles in IA of 32x32 pixels. Despite the low particle image density the detected spurious vectors resulted to be only about 2% for IA of 8x8 pixels, while no spurious vectors at all were detected for IA of 32x32 pixels. Values of ε_{Δ^2} for $N = 1,\ 5,\ 9$ and 50 are shown in Figure 9. As expected the use of a low particle density (LPD) background affected the accuracy of both BOS and EBOS techniques, compare Figure 9 and Figure 7. Nevertheless when using IA of 8x8 pixels EBOS showed a ε_{Δ^2} about 40% smaller then BOS (i.e. $N = 1$ in Figure 9). On the other side a very small difference between the two ε_{Δ^2} (about 8%) is observed using IA of 32x32 pixels. Also when using the LPD background $N = 5$ allows to achieve almost the maximum reduction in ε_{Δ^2}, Figure 9.

All the reported results support the conclusion that EBOS is able to reduces the displacement uncertainty as respect to BOS when both use the same IA size, stated differently EBOS can achieve the same or slightly lower uncertainty of BOS but using smaller IA size. Thus the EBOS technique is most advantageous to use when a small interrogation area size is required. When the signal to noise ratio (SNR) of the cross-correlation is high, i.e. let's say when the IA contains at least 10 particles, EBOS provides a very small improvement respect to BOS. Finally EBOS using images of the background pattern at 5 different positions is able to achieve almost the smallest mean error.

6. Conclusion

This work describes a technique able to reduce the uncertainty of the BOS techniques. The proposed technique doesn't make use of any temporal or spatial filter and we named it Enhanced BOS (EBOS). The EBOS technique uses N undistorted images of a single grey-scale background pattern,

each image is acquired with the background pattern at a slightly different position respect to a fixed reference one. The N undistorted background images are cross-correlated with a single image of the distorted background, eventually the resulting displacement maps are averaged together. The average procedure reduces the uncertainty of the displacement estimate. The EBOS technique could be coupled with optical flow algorithms, anyhow we limited our analysis to the cross-correlation technique. To compare EBOS and BOS they were both applied to the same test case. A displacement field was generated by rigidly rotating the background pattern around an axis perpendicular to the background plane. To make a correct comparison, the same image of the rotated background was analyzed by BOS and EBOS. For EBOS the undistorted background images were taken by displacing the background according to a regular square grid, in the image plane the absolute maximum background displacement was about 1.5 pixels. The results evidenced that when using the same IA size the EBOS gives a smaller displacement error respect to BOS. On the other side EBOS achieves the same mean errors of BOS but using IA of a factor four (area ratio) smaller than BOS. The EBOS technique provides quite small improvement respect to BOS when the SNR of the cross-correlation is high, i.e. let's say when the number of particle images contained in a IA is may be at least $5-10$. Finally EBOS using images of the background pattern at 5 different positions is able to achieve almost the smallest mean error.

References

[1] Dalziel S B, Hughes G O and Sutherland B R 2000 Whole-field density measurements by "synthetic schlieren" Exp. Fluids 28 322–35
[2] Raffel M, Richard H and Meier G E A 2000 On the applicability of background oriented optical tomography for large scale aerodynamic investigations Exp. Fluids 28 477–81
[3] Raffel M 2015 Background-oriented schlieren (BOS) techniques Exp. Fluids 56 1–17
[4] Merzkirch W 1987 Flow visualization (Orlando, Florida: Academic Press, Inc.)
[5] Elsinga G E, Van Oudheusden B W, Scarano F and Watt D W 2004 Assessment and application of quantitative schlieren methods: Calibrated color schlieren and background oriented schlieren Exp. Fluids 36 309–25
[6] Vinnichenko N A, Znamenskaya I A, Glazyrin F N and Uvarov A V 2011 Study of Background Oriented Schlieren Method Accuracy By Means of Synthetic Images Analysis 22nd International Symposium on Transport Phenomena pp 1–12
[7] Cozzi F, Göttlich E, Angelucci L, Dossena V and Guardone A 2017 Development of a background-oriented schlieren technique with telecentric lenses for supersonic flow J. Phys. Conf. Ser. 778 012006
[8] Atcheson B, Heidrich W and Ihrke I 2009 An evaluation of optical flow algorithms for background oriented schlieren imaging Exp. Fluids 46 467–76
[9] Hargather M J and Settles G S 2010 Natural-background-oriented schlieren imaging Exp. Fluids 48 59–68
[10] Richard H and Raffel M 2001 Principle and applications of the background oriented schlieren (BOS) method Meas. Sci. Technol. 12 1576–85
[11] Clem M M, Zaman K B M Q, Fagan A F and Glenn N 2012 Background Oriented Schlieren Applied to Study Shock Spacing in a Screeching Circular Jet 50th AIAA Aerosp. Sci. Meet. 1–12
[12] Kindler K, Goldhahn E, Leopold F and Raffel M 2007 Recent developments in background oriented Schlieren methods for rotor blade tip vortex measurements Exp. Fluids 43 233–40
[13] Bauknecht A, Merz C B, Landolt A, Meier A H and Raffel M 2013 Blade tip vortex detection in maneuvering flight using the Background Oriented Schlieren (BOS) technique AHS 69th Annu. Forum Technol. Disp. "Advancing Vert. Flight Technol. Demanding Environ. 1–13
[14] Cozzi F, Colombo L P M, Lucchini A, Coghe A, Muzzio A and Pacini F 2010 Background Oriented Schlieren characterization of the thermal boundary layer over a vertical heated plate in free convection pp 1–6

[15] Ota M, Leopold F, Noda R M K 2015 Improvement in spatial resolution of background-oriented schlieren technique by introducing a telecentric optical system and its application to supersonic flow Exp. Fluids 56 48
[16] Venkatakrishnan L and Suriyanarayanan P 2009 Density field of supersonic separated flow past an afterbody nozzle using tomographic reconstruction of BOS data Exp. Fluids 47 463–73
[17] Hartmann U, Adamczuk R and Seume J R 2015 Tomographic Background Oriented Schlieren Applications for Turbomachinery AIAA Aerosp. Sci. Meet. 5 2015–1690
[18] Klemkowsky J N, Fahringer T W, Clifford C J, Bathel B F and Thurow B S 2017 Plenoptic background oriented schlieren imaging Meas. Sci. Technol. 28 095404
[19] Leopold F 2007 The Application of the Colored Background Oriented Schlieren technique (CBOS) to free-flight and in-flight measurements ICIASF Record, International Congress on Instrumentation in Aerospace Simulation Facilities
[20] Leopold F, Ota M, Klatt D and Maeno K 2013 Reconstruction of the Unsteady Supersonic Flow around a Spike Using the Colored Background Oriented Schlieren Technique J. Flow Control. Meas. Vis. 01 69–76
[21] Sourgen F, Leopold F and Klatt D 2012 Reconstruction of the density field using the Colored Background Oriented Schlieren Technique (CBOS) Opt. Lasers Eng. 50 29–38
[22] Schröder A, Over B, Geisler R, Bulit A, Schwane R and Kompenhans J 2009 Measurements of density fields in micro nozzle plumes in vacuum by using an enhanced tomographic background oriented schlieren (BOS) technique 9th International symposium on measurement technology and intelligent instruments, Saint-Petersburg pp 1-272 1-276
[23] Michaelis D, Neal D R and Wieneke B 2016 Peak-locking reduction for particle image velocimetry Meas. Sci. Technol. 27 104005
[24] Adrian R J and Westerweel J 2011 Particle Image Velocimetry
[25] Raffel M, Willert C E, Scarano F, Kähler C J, Wereley S T and Kompenhans J 2018 Particle Image Velocimetry: A Practical Guide (Cham: Springer International Publishing)